

## Atomic Force Microscopy Characterization of Room-Temperature Adlayers of Small Organic Molecules through Graphene Templating

Peigen Cao,<sup>†</sup> Ke Xu,<sup>†,‡</sup> Joseph O. Varghese,<sup>†</sup> and James R. Heath<sup>\*,†</sup><sup>†</sup>Kavli Nanoscience Institute and Division of Chemistry and Chemical Engineering, California Institute of Technology, MC 127-72, Pasadena, California 91125, United States<sup>‡</sup>Department of Chemistry and Chemical Biology, Harvard University, 12 Oxford Street, Cambridge, Massachusetts 02138, United States

## S Supporting Information

**ABSTRACT:** We report on the use of graphene templating to investigate the room-temperature structure and dynamics of weakly bound adlayers at the interfaces between solids and vapors of small organic molecules. Monolayer graphene sheets are employed to preserve and template molecularly thin adlayers of tetrahydrofuran (THF) and cyclohexane on atomically flat mica substrates, thus permitting a structural characterization of the adlayers under ambient conditions through atomic force microscopy. We found the first two adlayers of both molecules adsorb in a layer-by-layer fashion, and atomically flat two-dimensional islands are observed for both the first and the second adlayers. THF adlayers form initially as rounded islands but, over a period of weeks, evolve into faceted islands, suggesting that the adlayers possess both liquid and solid properties at room temperature. Cyclohexane adlayers form crystal-like faceted islands and are immobile under the graphene template. The heights of the second adlayers of THF and cyclohexane are measured to be  $0.44 \pm 0.02$  and  $0.50 \pm 0.02$  nm, respectively, in good agreement with the layer thicknesses in the monoclinic crystal structure of THF and the Phase I "plastic crystal" structure of cyclohexane. The first adlayers appear slightly thinner for both molecules, indicative of interactions of the molecules with the mica substrate.

The first layers of organic molecules adsorbed to solid surfaces often determine the physics and chemistry of both the adsorbate and the substrate and, thus, play a crucial role in many applications, including, for example, heterogeneous catalysis, corrosion, adhesion, lubrication, and environmental control.<sup>1–3</sup> For instance, the adsorption of volatile organic molecules on ambient surfaces plays an important role in determining the environmental fate of airborne organic pollutants.<sup>2</sup>

However, most knowledge of adsorption processes has been gained from macroscopic measurements on large areas of surfaces, which provide limited information on the microscopic structures of adlayers. In particular, the structures of adlayers at the interfaces between solids and vapors of small organic molecules are poorly understood at ambient temperatures. The reasons are twofold. First, organic compounds capable of forming vapors at room temperatures are volatile, and so molecularly thin adlayers quickly evaporate away in the vacuum environments required by many surface characterization techniques.

Second, when vacuum is not required, the microscopic structure of the adlayers is still difficult to probe due to the mobile nature of small molecules on surfaces, although certain area- and time-averaged properties can be determined (e.g., the averaged thickness of adlayers<sup>4</sup>).

Previous experimental work on the room-temperature structures of weakly bound organic molecule adlayers (or molecularly thin films) on solids has largely been limited to nonvolatile molecules (boiling point  $\gg \sim 250$  °C) with high molecular weight (number of carbon atoms  $\gg 10$ ).<sup>5–11</sup> Such adlayers are typically obtained through coating from a solution phase and so differ from adlayers in equilibrium with a vapor. Alternatively, adlayers of small organic molecules have been studied at low temperatures ( $T \ll 200$  K), where the vapor pressure and mobility of molecules are drastically reduced.<sup>1,3,12,13</sup> However, adlayer structures are found to be highly temperature-dependent,<sup>3,12</sup> and thus the low- $T$  results cannot be directly compared with the room-temperature vapor adsorption one encounters in everyday life.

Here we report on the use of graphene sheets as an ultrathin template for the atomic force microscopy (AFM) characterization of the room-temperature structures of the adlayers at the interfaces between mica surfaces and vapors of small organic molecules. We previously demonstrated how graphene templating can be employed to probe the structure of water adlayers on mica under ambient conditions.<sup>14</sup> Here, we show that graphene, albeit only one-atom thick, can prevent the evaporation of molecularly thin adlayers of volatile small organic molecules and slows down, but does not fully prevent, the motions of the adsorbed molecules on the solid surface, thus allowing observation of both the *structure* and *dynamics* of the adlayers at room temperature. The small organic molecules, tetrahydrofuran (THF) and cyclohexane, representing the two classes of polar and nonpolar organic solvents, were investigated and compared with water.

Figure 1a illustrates the graphene templating technique. Samples were prepared at room temperature ( $\sim 22$  °C) and a relative humidity of  $< 2\%$ , under which the adsorption of water on mica surfaces can be neglected.<sup>14</sup> Freshly cleaved mica surfaces were brought into contact with organic vapors and allowed to equilibrate for  $\sim 1$  min. The partial pressure of organic molecules at the mica surface, which determines the surface coverage at

Received: September 22, 2010

Published: February 4, 2011

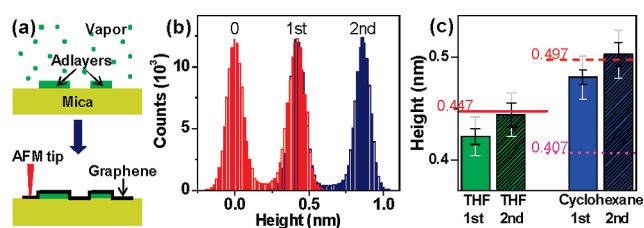


**Figure 1.** Graphene templating illustration (a) and representative measurements of adsorbed adlayer thicknesses (b,c). (b) THF adlayer heights, from two AFM images, at the borders between 0 and 1 (red) and 1 and 2 (blue) adlayers. The two distributions are overlaid according to the peak centers of the first adlayer. The heights for the first and second adlayers are respectively determined to be 0.420 and 0.446 nm (c) Statistics of the measured heights for the first and second adlayers of THF and cyclohexane on mica, obtained from  $\sim 10$  samples for each adlayer. The indicated uncertainties (95% confidence) are for when the systematic error in height calibration is excluded (black) and included (gray). Red lines mark the layer heights in the bulk crystals of THF (monoclinic) and cyclohexane (Phase I) that are in agreement with our data. The pink dotted line marks the layer height for a different crystal phase (Phase II) of the cyclohexane crystal and is in clear disagreement with our data.

equilibrium, was adjusted by varying the distance between the vapor source and the mica. Graphene sheets were deposited onto the mica, sealing and preserving the adlayer structures. Samples were then imaged with AFM under ambient conditions. See Supporting Information for experimental details. Adlayer heights in each sample were determined by scanning over small ( $\sim 200$  nm) areas across adlayer borders and plotting the distribution of all height values within the AFM images (Figure 1b). The final heights reported for THF and cyclohexane adlayers were summarized from the height values thus obtained from  $\sim 10$  different images (Figure 1c).

Figure 2 presents AFM images of monolayer graphene sheets deposited on mica surfaces that were in equilibrium with THF vapors. Atomically flat islands are observed across all graphene sheets. No such structures are observed on mica surfaces that are not covered by graphene. Phase images,<sup>14</sup> which are more reflective of the local chemical properties of the surface rather than the topography,<sup>15</sup> indicate that the observed flat islands are THF adlayers trapped under the graphene, similar to the case of water adlayers in our previous study.<sup>14</sup> The numbers of THF adlayers, as labeled in Figure 2, were determined from measured heights and careful tracing of the extreme edges of graphene sheets, where the adlayers under graphene tend to evaporate and leave the graphene in direct contact with the bare mica.<sup>14</sup>

Similar to what was found for water,<sup>14</sup> a layer-by-layer growth mechanism is observed for the first two adlayers of THF molecules: the second adlayer forms after the first adlayer is completed (Figure 2d,e and Figure S2), and two-dimensional (2D) flat islands are observed for both layers, similar to the Frank–van der Merwe growth mechanism in hetero-epitaxy.<sup>16</sup> No molecularly flat, island-like structures are seen beyond the second adlayer; droplets are observed to coexist with both the first and second adlayers. This general mechanism, however, is not universal. Different behavior is observed for water adlayers adsorbed on trimethylchlorosilane-functionalized ( $\text{H}_2\text{O}$  contact angle  $\sim 40^\circ$ ) mica. The adlayer structures that initially adsorb, as observed via graphene templating, are three-dimensional nanodroplets only, with no obvious crystalline structure (Figure S6).

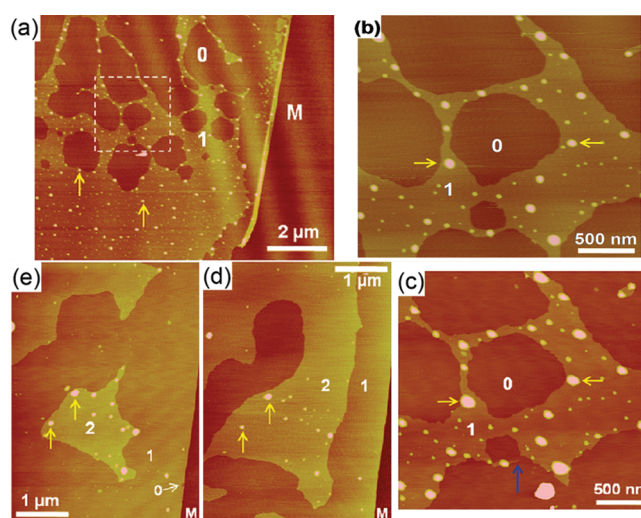


**Figure 2.** AFM images (labeled clockwise from top left) of graphene-templated THF adlayers reveal both structural and dynamical information. M labels the mica surface, and 0, 1, and 2 label regions where monolayer graphene is on top of 0, 1, and 2 adlayers of THF, respectively. Yellow arrows point to droplets. (a, b, and d) were taken within a few hours after graphene sheets were deposited; (c and e) were after storing under ambient conditions. (a) The case in which the trapped adlayer is a submonolayer. (b) Zoom-in of the square in (a). (c) Same area as (b) after 2 months. (d) Another sample showing the second THF adlayer on top of the first. (e) Same area as (d) after 2 months. Defects at the graphene edge (not shown) provided reference points for aligning the images.

Those results indicate multiple types of adlayer growth mechanisms can be achieved via chemical modification of the underlying mica substrate and can be preserved and imaged using graphene templating.

Figure 2a,b present the case in which the trapped adlayer is a submonolayer. Large, interconnecting islands coexist with areas where no adlayer is present. At low surface coverage, the adlayers tend to form narrow “necks” as opposed to isolated small islands (Figure S7). This contrasts with what is seen for submonolayers of water, where isolated and scattered small islands, typically  $\sim 10$  nm in lateral size, are observed<sup>14</sup> (see also Figure S5). This result suggests that, relative to water, THF molecules interact more weakly with the mica surface.

The boundaries of the islands formed by the first THF adlayers often appear rounded (Figure 2a,b). Similar boundaries are also observed at the missing edges of full monolayers (Figure S2). These results suggest that the first THF adlayer has some liquid-like characteristics. The second adlayers (Figure 2d) exhibit both rounded and faceted boundaries. As will be discussed below, the rounded boundaries of THF adlayers become increasingly faceted over time, suggesting, again, that these adlayers possess both liquid and solid properties at room temperature. These results contrast with water, for which both the first and second adlayers appear ice-like at room temperature, and are characterized by faceted boundaries with preferred angles of  $\sim 120^\circ$ .<sup>14,17,18</sup>

The heights of the first and second THF adlayers on the mica surface were measured, across  $\sim 10$  samples, to be  $0.42 \pm 0.02$  and  $0.44 \pm 0.02$  nm, respectively (Figure 1c). The height of the second adlayer is in agreement with the layer thickness in THF crystals: THF crystallizes in the monoclinic space group  $C2/c$ ,



and the layer thickness in the  $b$  direction is  $b/2 = 0.447$  nm (Figure 1c).<sup>19–21</sup> In this direction, THF molecules “stand up” with the oxygen atoms in the rings alternatively pointing toward and away from the substrate.<sup>21</sup> This also corresponds to the polarity direction for THF molecules. The height of the first adlayer is statistically thinner than the second adlayer: when the (systematic) uncertainty in height calibration is ignored, the heights of the first and second THF adlayers can be expressed as  $0.423 \pm 0.008$  and  $0.444 \pm 0.012$  nm, respectively. This result suggests that the first adlayers may be slightly tilted due to interactions with the substrate (Figure 4a,b), a phenomenon often encountered in self-assembled monolayers.<sup>22</sup>

Although the graphene-templated THF adlayers are stable over time scales of hours (e.g., the same structures are observed for images taken at different magnifications over periods of several hours), noticeable structural changes are observed over the time scale of weeks. This result is in contrast to graphene-templated water adlayers, which are stable for at least months under ambient conditions (Figure S5).<sup>14</sup> In most cases, the THF adlayers shrink in lateral dimensions to form droplets (Figure 2c,e). Narrow “necks” in the adlayers thus tend to break (blue arrow in Figure 2c). The boundaries of the THF adlayers also often adopt facets during the reorganization (Figure 2e). These observations are reminiscent of the coalescence of molecularly thin clusters/islands often encountered during the postdeposition relaxation processes in thin film deposition.<sup>23–25</sup> In our case, adlayers are sealed under graphene, so the vapor-adlayer equilibrium is removed for the otherwise volatile molecules. The adlayers thus relax in a manner that is similar to deposited nonvolatile thin films. We note that after the adlayers are allowed to relax for sufficiently long periods, reverse processes, in which droplets shrink in size to form larger adlayer islands, are also occasionally observed (Figure S7). Such reversible transitions are likely due to thermal fluctuations and are consistent with the idea that the adlayer structures observed here are within a few  $k_B T$  of energy.

The observations on the THF adlayers imply both liquid-like and crystalline characteristics at room temperature. This is remarkable since room temperature is  $\sim 130$  K higher than the bulk melting point of THF ( $-108.4$  °C). The coexistence of solid-like and liquid-like layers have been recently observed for the ionic liquid Bmim-PF<sub>6</sub> on mica surfaces.<sup>26</sup> However, the melting point of Bmim-PF<sub>6</sub> ( $6.6$  °C) is close to room temperature, and the liquid-like and solid-like structures observed in Bmim-PF<sub>6</sub> films, which are of unknown thicknesses,<sup>26</sup> likely only reflect the differences between bulk and adlayer properties. The faceted yet mobile adlayers we observed have not been previously reported. A possibility is that the THF adlayers are in a “hexatic” phase that is between the solid and liquid phases. In three dimensions, liquid–solid transitions are necessarily first-ordered and abrupt; for 2D systems the liquid–solid transition may occur continuously, through the intermediate “hexatic” phase, and over a wide temperature range.<sup>27–29</sup>

Figure 3 presents AFM images of monolayer graphene deposited on mica surfaces that were in equilibrium with cyclohexane vapors at room temperature. Again, a layer-by-layer growth mechanism is observed for cyclohexane adlayers, and atomically flat 2D islands are observed for both the first and the second adlayers. The surface coverage of cyclohexane on the mica surface is usually low, and so the second adlayer was only occasionally observed, typically surrounding droplets that are likely attracted by surface defects (Figure S8). This result

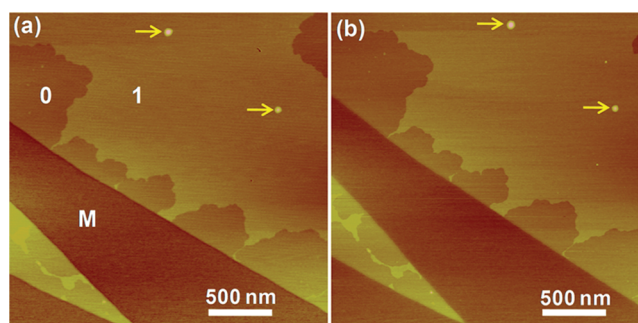


**Figure 3.** AFM images of graphene-templated cyclohexane adlayers. M labels the mica surface, and 0 and 1 label regions where monolayer graphene is on top of 0 and 1 adlayers of cyclohexane, respectively. Yellow arrows point to droplets. (a) A typical image of graphene-templated submonolayer cyclohexane adlayer, taken within a few hours after graphene was deposited. (b) The same area, but imaged after the sample was stored at ambient conditions for 2 months.

possibly reflects the weaker interaction between the nonpolar cyclohexane molecules and the mica surface.

Similar to the case of THF, but different from water, cyclohexane adlayers form large, continuous islands on mica (see also Figure S4), indicating weak molecule–substrate interactions. On the other hand, similar to the case of water but different from THF, the boundaries of all cyclohexane adlayers appear faceted, suggesting the adlayers are crystal-like at room temperature. In addition, the graphene-templated cyclohexane adlayers are stable for months without noticeable structural changes (Figures 3b and S4), again indicating that the adlayers are solid-like at room temperature. The crystallinity of the cyclohexane adlayers, relative to THF adlayers, is likely due to the large difference in melting points ( $6.7$  °C vs  $-108.4$  °C) and suggests that the interaction between adsorbed molecules plays an important role in determining the adlayer structure.

The heights of the first and second cyclohexane adlayers on the mica surface, across different samples, are measured to be  $0.48 \pm 0.02$  and  $0.50 \pm 0.02$  nm, respectively (Figure 1c). These values are in good agreement with the layer thickness of the phase I crystal structure of cyclohexane. Phase I is the stable phase for bulk cyclohexane between 279.8 and 186 K. The unit cell is face-center cubic (fcc) with  $a = 0.861$  nm.<sup>30,31</sup> The layer thickness in the (111) direction (i.e., a close-packed hexagonal single layer; Figure 4c) is thus  $a/\sqrt{3} = 0.497$  nm (Figure 1c). Previous low-energy electron diffraction (LEED) studies<sup>12,13</sup> over large areas of cyclohexane adlayers on Pt(111) and Ag(111) surfaces indicated that, for  $T < \sim 200$  K, cyclohexane adsorbs as a monoclinic phase, which is consistent with the phase II crystal structure. That structure is known to be stable for  $T < 186$  K in bulk. According to the phase II arrangement, the cyclohexane rings would lie roughly parallel to the substrate,<sup>12,13</sup> and the layer thickness should be  $\sim c/2 \sin \beta = 0.407$  nm.<sup>30</sup> That value is significantly smaller than the adlayer heights we measured (Figure 1c). No LEED patterns were observed in previous studies for  $T > \sim 200$  K, where cyclohexane adlayers evaporated in vacuum.<sup>12,13</sup> Thus, our results suggest, at room temperature, cyclohexane adlayers crystallize as phase I (Figure 4c). Phase I of cyclohexane is a plastic crystal, meaning that although molecules form ordered crystal lattices, they are still free to rotate about the lattice points.<sup>30,31</sup> The layer height is larger than for the case of phase II, in which all molecules lie “flat” on the substrate. Similar

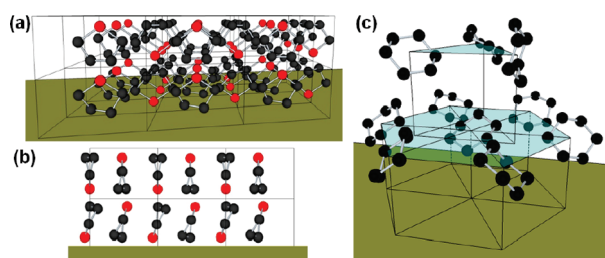


**Figure 4.** Possible structural models for THF and cyclohexane adlayers. Black and red balls represent carbon and oxygen atoms, respectively. Hydrogen atoms are omitted for clarity. (a,b) Possible structure of the first two adlayers of THF, basing on the monoclinic crystal structure of THF. (a) Perspective view. (b) Side view. The first adlayer may be tilted due to molecule–substrate interactions. (c) Instantaneous view of the possible structure of the first two adlayers of cyclohexane. The structure is based on the (111) direction of the fcc lattice of the phase I “plastic crystal” structure of cyclohexane. Each molecule is free to rotate about its center, and so this view represents one instantaneous snapshot. The rotational freedom may be lower for the first adlayer.

to the case of THF, and neglecting the systematic uncertainty in height calibration, the height of the first adlayer of cyclohexane ( $0.480 \pm 0.007$ ) is statistically thinner than the second adlayer ( $0.503 \pm 0.012$  nm) (Figure 1c). One possibility is that interactions with the substrate may restrain the rotation of first adlayer cyclohexane molecules on the mica surface (Figure 4c).

We have reported on the room-temperature structures and dynamics of weakly bound adlayers at the interfaces between solids and vapors of small organic molecules by using graphene templating. We found cyclohexane adlayers on mica are crystal-like at room temperature, whereas THF adlayers possess liquid and solid properties. The heights of the second adlayers of THF and cyclohexane agree with the layer thicknesses in the monoclinic crystal structure of THF and the phase I “plastic crystal” structure of cyclohexane. The first adlayers of both molecules appear slightly thinner, indicative of molecule/mica interactions. A layer-by-layer growth mechanism has been consistently observed for the first two adlayers of water, THF, and cyclohexane molecules on freshly cleaved mica. Previous studies indicated that, for nonvolatile, large organic molecules, layer-by-layer spreading also occurs on flat substrates, for molecules that are both solid<sup>7,9,10</sup> and liquid<sup>5,6,26</sup> at room temperature. The consistency across different systems suggest that the layer-by-layer mechanism may be broadly applicable for molecular adsorbates on many atomically flat surfaces.

An outstanding question involves the influence of the graphene on the adlayer structure. Our findings indicate that graphene templating permits unprecedented high resolution views of weakly bound molecular adlayers, and the resultant data are wholly consistent with previous findings. This indicates that, at least for some systems, graphene templating provides a relatively innocent structural probe. However, it is likely that quantum mechanical calculations will be required to fully address this question and that the answer will be system-dependent.

## ■ ASSOCIATED CONTENT

**Supporting Information.** Experimental details and supplementary figures. This material is available free of charge via the Internet at <http://pubs.acs.org>.

## ■ AUTHOR INFORMATION

Corresponding Author

heath@caltech.edu

## ■ ACKNOWLEDGMENT

We thank Wan Li (Cornell) for helpful discussions. We also thank G. Rossman for assistance in using the Micro Raman spectrometer. This work was funded by the Department of Energy (DE-FG02-04ER46175). J.O.V. acknowledges support from a National Science Foundation graduate fellowship.

## ■ REFERENCES

- (1) Weaver, J. F.; Carlsson, A. F.; Madix, R. J. *Surf. Sci. Rep.* **2003**, *50*, 107.
- (2) Goss, K. U. *Crit. Rev. Environ. Sci. Technol.* **2004**, *34*, 339.
- (3) Bruch, L. W.; Diehl, R. D.; Venables, J. A. *Rev. Mod. Phys.* **2007**, *79*, 1381.
- (4) Beaglehole, D.; Christenson, H. K. *J. Phys. Chem.* **1992**, *96*, 3395.
- (5) Xu, L.; Salmeron, M.; Bardon, S. *Phys. Rev. Lett.* **2000**, *84*, 1519.
- (6) Xu, L.; Ogletree, D. F.; Salmeron, M.; Tang, H. A.; Gui, J.; Marchon, B. *J. Chem. Phys.* **2000**, *112*, 2952.
- (7) Lazar, P.; Schollmeyer, H.; Riegler, H. *Phys. Rev. Lett.* **2005**, *94*, 116101.
- (8) Riegler, H.; Kohler, R. *Nat. Phys.* **2007**, *3*, 890.
- (9) Trogisch, S.; Simpson, M. J.; Taub, H.; Volkmann, U. G.; Pino, M.; Hansen, F. Y. *J. Chem. Phys.* **2005**, *123*, 154703.
- (10) Cisternas, E. A.; Corrales, T. P.; del Campo, V.; Soza, P. A.; Volkmann, U. G.; Bai, M. J.; Taub, H.; Hansen, F. Y. *J. Chem. Phys.* **2009**, *131*, 114705.
- (11) Giancarlo, L. C.; Flynn, G. W. *Annu. Rev. Phys. Chem.* **1998**, *49*, 297.
- (12) Firment, L. E.; Somorjai, G. A. *J. Chem. Phys.* **1977**, *66*, 2901.
- (13) Firment, L. E.; Somorjai, G. A. *J. Chem. Phys.* **1978**, *69*, 3940.
- (14) Xu, K.; Cao, P. G.; Heath, J. R. *Science* **2010**, *329*, 1188.
- (15) Garcia, R.; Perez, R. *Surf. Sci. Rep.* **2002**, *47*, 197.
- (16) Herman, M. A.; Richter, W.; Sitter, H. *Epitaxy: Physical Principles and Technical Implementation*; Springer: Berlin, 2004.
- (17) Hu, J.; Xiao, X. D.; Ogletree, D. F.; Salmeron, M. *Science* **1995**, *268*, 267.
- (18) Verdager, A.; Sacha, G. M.; Bluhm, H.; Salmeron, M. *Chem. Rev.* **2006**, *106*, 1478.
- (19) David, W. I. F.; Ibberson, R. M. *Acta Crystallogr., Sect. C: Cryst. Struct. Commun.* **1992**, *48*, 301.
- (20) Luger, P.; Buschmann, J. *Angew. Chem., Int. Ed. Engl.* **1983**, *22*, 410.
- (21) Dziubek, K. F.; Jeczminski, D.; Katrusiak, A. *J. Phys. Chem. Lett.* **2010**, *1*, 844.
- (22) Ulman, A. *Chem. Rev.* **1996**, *96*, 1533.
- (23) Zinkeallmang, M.; Feldman, L. C.; Grabow, M. H. *Surf. Sci. Rep.* **1992**, *16*, 377.
- (24) Venables, J. A.; Spiller, G. D. T.; Hanbucken, M. *Rep. Prog. Phys.* **1984**, *47*, 399.
- (25) Evans, J. W.; Thiel, P. A.; Bartelt, M. C. *Surf. Sci. Rep.* **2006**, *61*, 1.
- (26) Liu, Y. D.; Zhang, Y.; Wu, G. Z.; Hu, J. *J. Am. Chem. Soc.* **2006**, *128*, 7456.
- (27) Strandburg, K. J. *Rev. Mod. Phys.* **1988**, *60*, 161.
- (28) Binder, K.; Sengupta, S.; Nielaba, P. *J. Phys.: Condens. Matter* **2002**, *14*, 2323.
- (29) Gasser, U.; Eisenmann, C.; Maret, G.; Keim, P. *ChemPhysChem* **2010**, *11*, 963.
- (30) Kahn, R.; Fourme, R.; Andre, D.; Renaud, M. *Acta Crystallogr., Sect. B: Struct. Commun.* **1973**, *B 29*, 131.
- (31) Shigematsu, K.; Hondo, H.; Kumagai, T.; Takahashi, Y. *Cryst. Growth Des.* **2009**, *9*, 4674.